Insights into bonding and hydrogen bond directionality in thioacetamide from the experimental charge distribution

Trevor W. Hambley,[a] David E. Hibbs,*[a] Peter Turner,[a] Siân T. Howard[b] and Michael B. Hursthouse[c]

[a] *Centre for Heavy Metals Research, School of Chemistry, University of Sydney, Sydney, NSW 2006, Australia. E-mail: d.hibbs@chem.usyd.edu.au; Fax: +61 (02) 9351 3329; Tel: +61 (02) 9351 7482*

[b] *Chemistry Department, Cardiff University, PO Box 912, Cardiff, UK CF3 3TB. E-mail: howardst@cf.ac.uk; Fax: +44 (0) 2924 874029; Tel: +44 (0) 2920 874000*

[c] *School of Chemistry, University of Southampton, Highfield, Southampton, UK SO17 1BJ. E-mail: m.b.hursthouse@soton.ac.uk; Fax: +44 (023) 80596723; Tel: +44 (023) 80596722*

Received (in Cambridge, UK) 15th October 2001, Accepted 20th November 2001
First published as an Advance Article on the web 8th January 2002

A multipole model of the charge density distribution in thioacetamide has been obtained using high-resolution single crystal X-ray diffraction data. Topological analysis of the total experimental charge density $\rho(\boldsymbol{r})$ and its Laplacian $-\nabla^2\rho(\boldsymbol{r})$ at the bond critical points reveals fine details of intra- and intermolecular bonding features.

Introduction

Although there have been two previous crystallographic studies of thioacetamide (CH_3CSNH_2),[1,2] these were low resolution structural studies, from which it was not possible to obtain any charge density information. The study by Jeffrey *et al.*[1] concentrated on the comparison of high-precision crystal structure analysis coupled with *ab initio* calculations to distinguish small structural differences between the two molecules in the asymmetric unit (related by a non-crystallographic centre of symmetry), including those arising from crystal-field effects. The authors concluded that the presence of hydrogen bonding in the crystal alone could not cause the discrepancy between observed and calculated bond lengths in the thioamide side-chain, with HF/3-21G and HF/3-21G* basis set calculations under- and over estimating the bond lengths, respectively. They concluded that van der Waals forces or dipole interactions must be the reason for the lack of agreement between the (solid state) experimental structure and the (gas phase) single molecule calculation. However, little mention was made of the possibility of the thioamide side chain existing as the zwitterionic form (Fig. 1).

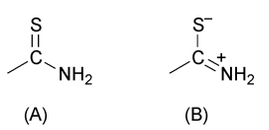

Fig. 1 Zwitterionic forms of the thioamido group; (A) amide form, (B) ionic form.

The study by Truter[2] addressed this possibility with conclusions drawn directly from inter-nuclear geometry. The conclusion drawn was that thioacetamide exists purely as the amide form (A). The current study was undertaken to determine experimentally the electron density distribution in thioacetamide, to clarify some of the outstanding inconsistencies in both the intra- and inter-molecular bonding characteristics.

Experimental

High-resolution low temperature X-ray diffraction data were collected using an Enraf Nonius FAST area detector diffractometer. Cell constants were obtained from the least squares refinement of 50 reflections located between 5.3 and 106.9° 2θ. Two reciprocal space data spheres were collected, with one sphere providing data between +3.0 and −52° 2θ, and a second for data between −37 and −110° 2θ. Data were collected at 100(2) K with omega scan increments of 0.20°, with the orientation matrix continually recalculated every 250 reflections. The intensities of 15 standard reflections collected in the overlap region did not change significantly during data collection, therefore no scaling correction was applied. Data reduction was carried out using the DREAM[3] program package. An analytical correction for absorption was carried out using SHELX-80.[4] The topological analysis of the experimental charge distribution used the XDPROP part of the XD program package.[5]

All gas phase DFT calculations were performed on the dimers with the GAUSSIAN98 program package[6] at the 6-311 ++G** level of theory at the crystal geometry, using the exchange functional of Becke in combination with correlation potential of Lee, Yang and Parr (BLYP).[7] The topological analyses of the theoretical data were based on the wave functions obtained from single point calculations using the same basis sets, and used the AIMPAC suite of programs.[8]

Multipole refinement

The crystal structure was determined in an earlier publication,[1] and the structural parameters therein formed the starting point for a high-order independent atom model (IAM) refinement where all atoms are treated as spherical. Bond lengths to hydrogen atoms were normalised to average neutron diffraction values,[9] with bond directions and isotropic temperature factors fixed at values obtained from the IAM refinement. For Csp^3–H, and N–H, the values were 1.097 and 1.032 Å respectively. Multipole refinement was carried out using the generalised scattering factor model based on the Hansen–Coppens formalism.[10] Refinements were carried out using the full-matrix least-squares program XDLSM, also part of the of the XD program package, which utilizes the well established rigid pseudoatom model.[10–12] For all refinements the quantity $\Sigma w(|F_o| - k|F_c|)^2$ was minimised with the statistical weight $w = \sigma - 2(F_o)$, using structure factors that met $F_o > 3\sigma(F_o)$.

DOI: 10.1039/b109353c

In a crystal the electron density $\rho(\boldsymbol{r})$ can be described by a sum of aspherical pseudoatoms with nuclear positions $\{\boldsymbol{R}_j\}$:

$$\rho(\boldsymbol{r}) = \Sigma_j \rho_j(\boldsymbol{r} - \boldsymbol{R}_j) \quad (1)$$

With the pseudoatomic density form of:

$$\rho_j(\boldsymbol{r}_j) = P_c\rho_c(\boldsymbol{r}_j) + \kappa'^3 P_v\rho_v(\kappa'\boldsymbol{r}_j) + \kappa'' P_{lm}\boldsymbol{R}_l(\kappa''\boldsymbol{r}_j)d_{lmp}(\theta_j,\varphi_j) \quad (2)$$

thus each pseudoatom is described by three components, core density, spherical valence density, and the deviation of the pseudoatom density from sphericity. The core and spherical valence density was composed of Hartree–Fock wave functions expanded over Slater type basis functions, with κ' (the expansion–contraction coefficient which modifies the radial distribution) being refined along with the valence population (P_v) fixed at 2 for first row atoms. The final term, again describing the deviation of the pseudoatom density from sphericity, is represented by deformation functions in the form of density-normalised spherical harmonics d_{lmp}.[10]

The Slater type function $N\boldsymbol{r}^{nl}\exp(-\kappa''\zeta\boldsymbol{r})$, forms the radial term ($\boldsymbol{R}_l$) for the deformation functions, with an additional radial screening parameter (κ'') being refined. The exponents nl of the Slater function were chosen so that the maximum of the radial function was at the density peak position ($r_{max} = (n_l/\zeta_l)$). The program FSTRUCT[13] was used to calculate theoretical structure factors from the DFT wave function, with the same Bragg reflections used in the experimental refinement, and these data were used to determine the best values of the Slater exponents. The temperature factors were set to unity, since it is only the static Born–Oppenheimer densities are needed for comparison with the corresponding static experimental density. These structure factors were then treated as observed data and refined with XDLSM in the same manner as the experimental data, but with no refinement of positional parameters, temperature factors or scale factor. The standard values of 4,4,4 (for dipoles, quadrupoles and octupoles) were found to give the best fit in this case. The value of ζ is taken from reference 11. The planarity of the molecules allows for the omission of hexadecapole functions on all atoms except for C(2) and C(2′). However, these higher functions had negligible population parameters and were also omitted. A constraint whereby the overall charge on the molecule was kept neutral was applied. In this refinement the expansion was truncated at the octupole level ($l_{max} = 3$) for heavy atoms while the asphericity of the hydrogen atoms was modelled with a single bond-directed dipole ($l_{max} = 2$). Separate κ' and κ'' were employed on all heavy atoms, although atoms that were chemically 'equivalent' had the same κ sets. Hydrogen κ' and κ'' were constrained to have the value 1.2, as obtained from theoretical studies.[14]

Given that there are two independent molecules in the asymmetric unit, this suggests at least two possible refinement strategies: (*a*) Both molecules treated independently, enabling comparison of their charge distributions and to interpret the observed differences in terms of intermolecular interactions within dimers. (*b*) The charge densities of the two independent molecules are averaged. Such a procedure forgoes any chance of studying how the molecules affect each others' charge distributions. However, it may be justified if the main aim is simply to obtain a high quality charge distribution for a single molecule, enabling conclusions to be drawn about both bonded and non-bonded electron pairs. In approach (*a*), sensible monopole charges with low SUs (0.05–0.07 *e*) were obtained, but an inspection of the residual density maps gave the first indication of the inadequacy of the model. The residual density in the plane of the molecule showed troughs (between −0.4 and −0.6 *e* Å^{-3}) at the nuclear positions and high peaks (0.2–0.4 *e* Å^{-3}) in the lone pair regions. Further, topological analysis of the resultant charge density of this refinement exhibited a number of deficiencies. In particular the C–N critical point values of ρ and $-\nabla^2\rho$ in molecules 1 and 2 differing considerably from each other, and the ellipticities (ε) of bonds to hydrogen atoms being unrealistically large. The agreement with the Density Functional Theory BLYP/6-311++G** calculated values of ρ and $-\nabla^2\rho$ was generally poor. The maps of the experimental $-\nabla^2\rho$ failed to recreate the contiguous region of density around the heavy atoms exhibited in the calculated maps, in particular sulfur, with large gaps and very diffuse density in the lone pair regions.

Approach (*b*) however, with the advantage of a larger N_{ref}/N_{var} ratio, and correspondingly improved refinement statistics, appeared to be the only approach which results in a reliable charge density distribution in good agreement with DFT calculations. In this method the multipole populations of the same atom in each independent molecule are constrained to be equal, in addition to this a plane of symmetry was imposed on the heavy atoms S(1), C(1) and N(1), such that multipoles with an odd *z* component are forced to be zero. This refinement converged smoothly with no large least-squares correlation coefficients, all bonds easily satisfying Hirshfeld's rigid-bond criterion.[15]

Table 1 Final multipole refinement statistics for thioacetamide

Formula	C_2H_5NS
Molecular mass	75.13
Crystal size/mm	0.20 × 0.18 × 0.17
Temperature/K	100(2)
Crystal system	monoclinic
Space group	$P2_1/n$
a	7.030(1)
b	9.911(2)
c	11.019(5)
β	99.643(4)
Volume/Å^3	756.9(4)
Z	8
D_c/g cm^{-3}	1.319
Radiation	Mo-*Kα*; $\lambda = 0.71069$
Max ($\sin\theta/\lambda$)/Å^{-1}	1.23
Absorption coefficient/cm^{-1}	6.11
No. of reflections measured	14444
No. of unique reflections	2806
Index ranges	$-12 \le h \le 12$, $-19 \le k \le 19$, $-21 \le l \le 22$
R(int)	0.0201
Refined on	F^2
No. reflections $I > 2\sigma I$ (N_{ref})	2280
R(F)	0.0265
wR	0.0278
S	1.30
N_{ref}/N_{var}	45.6

Results

The final refinement statistics for the constrained refinement are given in Table 1, atomic labelling is given in Fig. 2 and

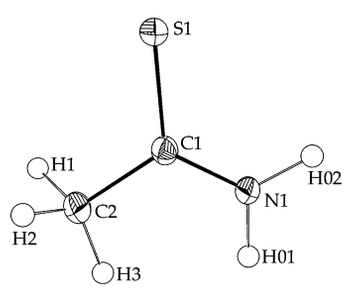

Fig. 2 Molecular structure of one molecule of thioacetamide. Ellipsoids are at 50% probability.

selected bond lengths and angles (including values from previous studies) are given in Table 2. Anisotropic displacement

Table 2 Selected bond lengths and angles for thioacetamide [Å, (°)]

Molecule 1		Molecule 2	
This study (X-ray data 100 K)			
S(1)–C(1)	1.681(3)	S(1′)–C(1′)	1.688(2)
N(1)–C(1)	1.316(4)	N(1′)–C(1′)	1.307(4)
C(1)–C(2)	1.502(3)	C(1′)–C(2′)	1.504(3)
N(1)–C(1)–C(2)	116.2(2)	N(1′)–C(1′)–C(2′)	116.1(2)
N(1)–C(1)–S(1)	122.9(2)	N(1′)–C(1′)–S(1′)	122.6(2)
C(2)–C(1)–S(1)	120.8(2)	C(2′)–C(1′)–S(1′)	121.3(2)
Ref. 1 (Neutron data 15 K)			
S(1)–C(1)	1.686(3)	S(1′)–C(1′)	1.690(8)
N(1)–C(1)	1.317(4)	N(1′)–C(1′)	1.316(7)
C(1)–C(2)	1.504(8)	C(1′)–C(2′)	1.502(1)
N(1)–C(1)–C(2)	116.5(1)	N(1′)–C(1′)–C(2′)	116.3(1)
N(1)–C(1)–S(1)	122.8(1)	N(1′)–C(1′)–S(1′)	122.5(1)
C(2)–C(1)–S(1)	120.8(1)	C(2′)–C(1′)–S(1′)	121.3(1)
Ref. 2 (X-ray data 298 K)			
S(1)–C(1)	1.710(8)	S(1′)–C(1′)	1.716(8)
N(1)–C(1)	1.324(11)	N(1′)–C(1′)	1.323(11)
C(1)–C(2)	1.497(11)	C(1′)–C(2′)	1.490(12)
N(1)–C(1)–C(2)	118.6(6)	N(1′)–C(1′)–C(2′)	116.7(6)
N(1)–C(1)–S(1)	121.7(6)	N(1′)–C(1′)–S(1′)	121.6(6)
C(2)–C(1)–S(1)	119.7(7)	C(2′)–C(1′)–S(1′)	121.7(7)

Table 3 Monopole charges and κ values

Atom	Monopole charge/*e*	κ'	κ''
S(1)	−0.72(3)	0.97(1)	0.96(5)
N(1)	−0.77(4)	0.96(1)	0.89(5)
C(1)	+0.37(5)	1.01(2)	0.99(3)
C(2)	−0.63(3)	0.96(3)	0.86(3)

parameters, fractional coordinates and multipole population coefficients are available as supplementary material. †

The values of κ' and κ'' for multipoles ($1 \leq l \leq 3$) for S(1), S(1′) refined to 0.97(1) and 0.96(5), indicating an expansion of the monopole and higher multipole terms in comparison to the free atom. Similarly for N(1), N(1′) 0.96(1) and 0.89(5), and C(2), C(2′) 0.96(3) and 0.86(3), while C(1), C(1′) 1.01(2) and 0.99(3) indicates a contraction of the monopole while the higher multipoles remain expanded. The dipole moment of the dimer is 0.9(2) D, with the individual dipole moments of each molecule being 9.0(1) D. This compares with 0.3 and 4.8 D from theoretical BLYP/6-311++G** calculations. Such an increase of the molecular dipole moment of ≈ 100% is not unprecedented.[16]

Fig. 3 shows the residual density in the plane defined by C(1)–S(1)–N(1), and is essentially the same for each of the two independent molecules. Fig. 4 shows the static deformation density in the same plane, while Fig. 5 and 6 show the experimental and theoretical Laplacian maps respectively. Again the Laplacian maps are essentially identical for each molecule, thus only one is shown. Table 3 reports monopole charges and the associated κ values.

Bond (3, −1) Critical Point data are presented in Table 4.

Table 5 details the hydrogen bonding present in the thioacetamide crystal, and Table 6 reports the CP analysis for these interactions. Table 7 reports the CP analysis for the lone pairs on sulfur.

† CCDC reference number 172905. See http://www.rsc.org/suppdata/p2/b1/b109353c/ for crystallographic files in .cif or other electronic format.

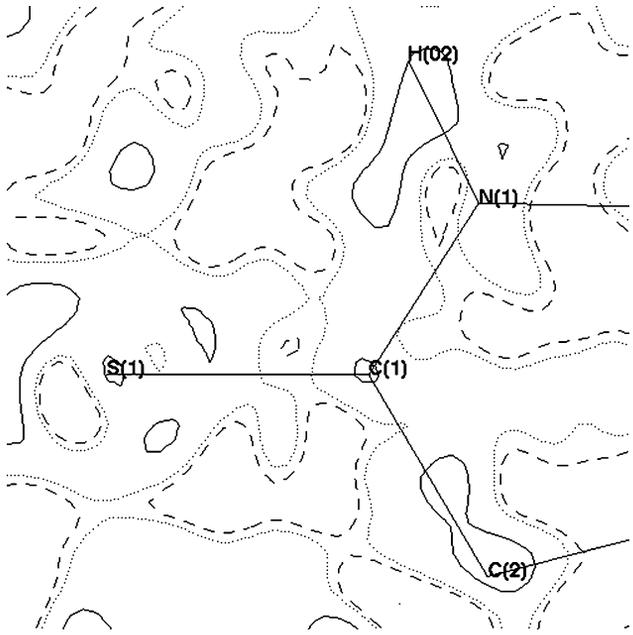

Fig. 3 Residual density in the S(1)–C(1)–N(1) plane. Contours (···) zero and (—) negative are at 0.1 *e* Å^{-3}.

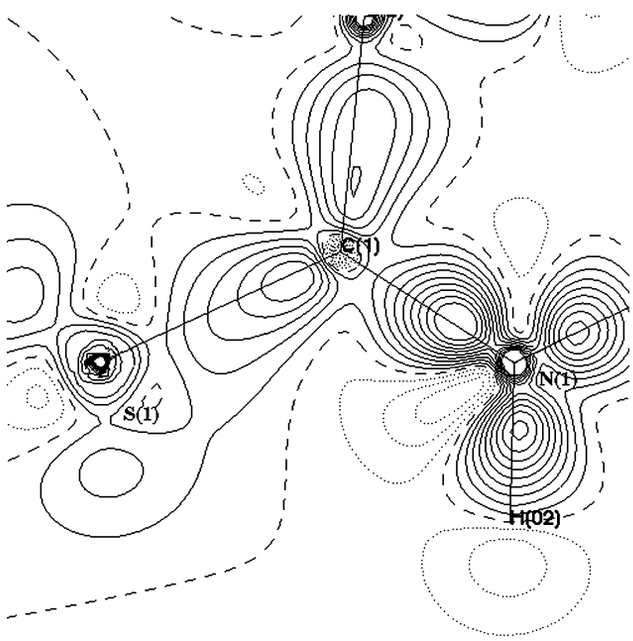

Fig. 4 Experimental static deformation density (—) zero and (···) negative contours. Contour level 0.1 *e* Å^{-3}.

Discussion

Thioacetamide (Fig. 2) crystallises in the centrosymmetric space group $P2_1/n$, with two molecules in the asymmetric unit, with a non-crystallographic centre of inversion between them, and the bond lengths and angles of this study do not differ significantly from those reported in the neutron structure determination.[1]

Comparison of experimental and theoretical charge distributions

Comparing the experimental CP data with the theoretical results we see that the agreement is good, although there is a tendency to overestimate the ellipticity values in the three C–H (methyl) bonds, and also ρ at the CPs is markedly underestimated with respect to theory. This is strongly indicative of rotation (or at least some libration) of the methyl group, as indeed was noted at 15 K by Jeffrey *et al*.

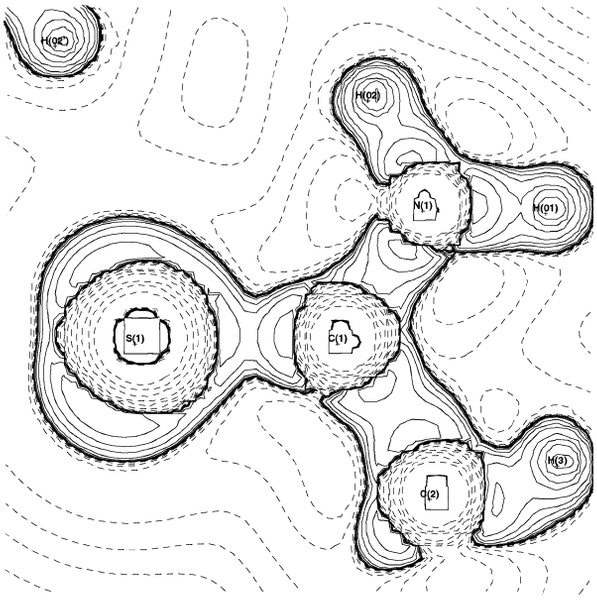

Fig. 5 Experimental Laplacian distribution in the S(1)–C(1)–N(1) plane, showing the S ⋯ H–N interaction.

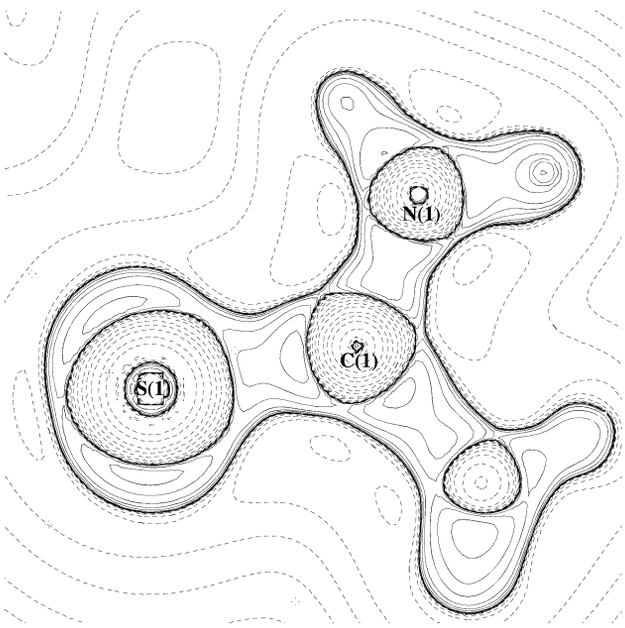

Fig. 6 Theoretical (BLYP/6-311++G**) Laplacian distribution in the S(1)–C(1)–N(1) plane.

From a purely structural viewpoint, the mean bond length for C(1)–C(2) is 1.503(2) Å, indicative of single bond between these atoms. The mean C(1)–S(1) bond length of 1.684(2) Å is in the range between typical C–S single bond (1.795 Å) and C=S double bond (1.615 Å) lengths. Similarly the mean C(1)–N(1) bond length of 1.312(2) Å is much shorter than the typical C–N single bond (1.47 Å), and very close to the typical C=N double bond value (1.30 Å). Moreover, the mean sum of bond angles at N(1) is 360.1°, *i.e.* a completely planar (sp^2-hybridised) nitrogen. These structural data therefore point to a strongly delocalised S–C–N system. Therefore an experimental charge density study was carried out to determine the extent of the conjugation.

Comparing the experimentally determined values with the calculated BLYP/6-311++G** results, we see that the agreement is good. A key observation with regard to the CP analysis is that the ellipticities of the S–C (0.11) and C–N (0.03) bonds, of key interest, are in quite good agreement with theory (0.18 and 0.03, respectively). This indicates conjugation in the S–C bond but little hyper-conjugation in the C–N bond. The theoretical and experimental values of ε provide a reasonably consistent picture, namely that the canonical form (A) of thioacetamide predominates in the solid state.

Table 4 Critical point (CP) data [a]

Bond	ρ/e Å^{-3}	$-\nabla^2\rho/e$ Å^{-5}	ε
S(1)–C(1)	1.53(1.42)	6.16(4.04)	0.11(0.18)
C(1)–C(2)	1.73(1.82)	14.79(18.90)	0.04(0.04)
C(1)–N(1)	2.32(2.35)	20.62(16.82)	0.03(0.03)
S(1′)–C(1′)	1.52(1.41)	7.80(3.70)	0.11(0.18)
C(1′)–C(2′)	1.72(1.81)	14.72(18.85)	0.04(0.03)
C(1′)–N(1′)	2.30(2.39)	20.24(16.48)	0.02(0.03)
N(1)–H(01)	1.77(2.23)	38.98(40.96)	0.03(0.05)
N(1)–H(02)	1.83(2.20)	48.10(47.47)	0.06(0.04)
N(1′)–H(01′)	1.78(2.24)	39.04(42.96)	0.03(0.05)
N(1′)–H(02′)	1.82(2.11)	47.45(48.40)	0.06(0.04)
C(2)–H(1)	1.55(1.86)	11.04(23.62)	0.19(0.03)
C(2)–H(2)	1.60(1.87)	12.54(23.70)	0.19(0.03)
C(2)–H(3)	1.61(1.86)	12.14(23.60)	0.08(0.01)
C(2′)–H(1′)	1.56(1.86)	10.10(23.49)	0.13(0.03)
C(2′)–H(2′)	1.57(1.88)	11.83(23.97)	0.20(0.02)
C(2′)–H(3′)	1.65(1.86)	14.12(23.45)	0.20(0.02)

[a] Values in parentheses are the BLYP/6-311++G** calculated values.

Table 5 Hydrogen bonding in thioacetamide [Å, (°)]

	d (N–H)	d (H–S)	d (N–S)	∠(NH ⋯ S)
H(01) ⋯ S(1′)[a]	1.023	2.358(3)	3.378(5)	175.81(9)
H(02) ⋯ S(1′)[b]	1.023	2.453(4)	3.420(7)	160.07(11)
H(01′) ⋯ S(1)[a]	1.023	2.379(7)	3.396(5)	173.68(10)
H(02′) ⋯ S(1)[b]	1.023	2.469(4)	3.474(3)	167.63(12)

[a] $(x, 0.5 - y, 0.5 - z)$. [b] (x, y, z).

Table 6 CP data for hydrogen bonds present in thioacetamide

	ρ/e Å^{-3}	$-\nabla^2\rho/e$ Å^{-5}	ε
S(1) ⋯ H(01′)	0.09	+1.082	0.10
S(1) ⋯ H(02′)	0.08	+1.030	0.09
S(1′) ⋯ H(01)	0.11	+1.342	0.08
S(1′) ⋯ H(02)	0.11	+1.416	0.10

Table 7 Lone pair (LP) (3,−3) critical point data for thioacetamide

Multipole refined			BLYP/6-311++G**	
Lone pair	$\nabla^2\rho$	d[a]	$\nabla^2\rho$	d[a]
S(1)LP1	−14.546	0.691	−12.126	0.692
S(1)LP2	−18.849	0.683	−12.162	0.691
S(1′)LP1	−14.566	0.691	−12.141	0.692
S(1′)LP2	−18.851	0.683	−12.168	0.691

[a] Distance from sulfur nucleus to LP centroid (Å).

Hydrogen bonding and the charge distribution

Each sulfur atom in thioacetamide donates two LPs in hydrogen bonds to amido protons of a molecule: (*a*) in an adjoining cell (*via* a 2_1 screw) and (*b*) between the two molecules in the asymmetric unit (Fig. 7). The hydrogen bonds link the molecules to form buckled layers, however there is no hydrogen bonding between the layers which have a separation of 3.5 Å. The topological analysis of these bonds is given in Table 6.

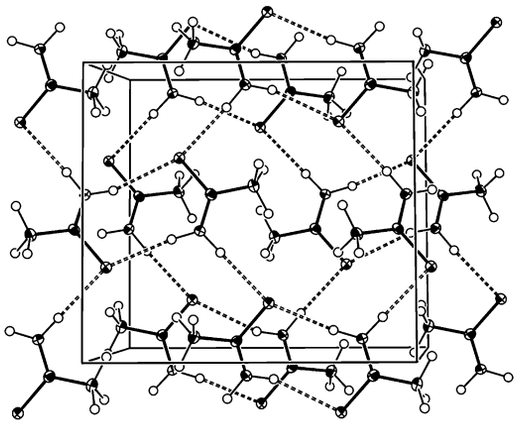

Fig. 7 Hydrogen bonds in thioacetamide.

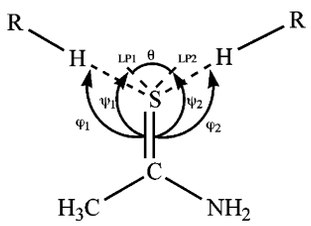

Fig. 8 Orientation of H-bonds and lone pairs in thioacetamide.

The values of the topology of the sulfur lone pairs are given in Table 7. The averaging procedure applied here guarantees that the values must be very similar between molecules 1 and 2, and thus it is impossible to determine the differences between any of the hydrogen bonds.

The *m* symmetry constraint on the sulfur multipoles means that LP1, LP2, S(1) and C(1) necessarily lie in a plane in the case of the experimental data, *i.e.* $\psi_1 + \psi_2 + \theta = 360.0°$ (Fig. 8). There is no such constraint on the theoretical LP positions; but intra- and inter-molecular interactions have only a very small effect on the planarity of the LP system: $\psi_1 + \psi_2 + \theta = 360.3$ and 359.7° respectively for the above theoretical data. Turning now to the experimental LP positions; on average, the angular positions of the LP's show a 10° discrepancy with respect to the theoretical values, but are nevertheless still realistic for a thiocarbonyl group. An average discrepancy in the radial distances of the LPs from the sulfur nuclei of 0.005 Å is found between experiment and theory. According to Carrol and Bader[17] the LP direction should effectively predict the direction of any hydrogen bond to it. Here the angular orientation φ of the hydrogen bonds is on average about 100°, which supports the observation of Platts *et al.* that hydrogen bonding to thiocarbonyl sulfur atoms is more perpendicular to the S–C bond than hydrogen bonds to carbonyl groups.[18] Despite the almost identical radial distances of the sulfur LPs from the sulfur nucleus, the values of $\nabla^2\rho$ are markedly different, *i.e.* the LP eclipsed with the NH_2 group has a higher concentration of electron density than the other. This might be attributed to hydrogen bonding, although in a theoretical study changes in LP properties of less than 1 % were observed. In a previous experimental charge density study,[19] such asymmetry in the two lone pairs of a carbonyl oxygen has been observed, and was apparently countered by the imposition of *mm2* site symmetry on this atom's multipoles.

Conclusions

Multipole refinement and subsequent topological analysis of the resulting charge distribution identified critical points (including those characteristic of intra-molecular bonding) in which the values of ρ and $-\nabla^2\rho$ agree closely with those calculated by Density Functional Theory. Properties at the bond critical points reveal fine details of inter- and intra-molecular interactions. It has been shown that experimental charge density studies can clarify issues related to both intra- and inter-molecular bonding interactions, and that the directionality of hydrogen bonding cannot be predicted solely by lone pair geometry. We believe that the ability of charge density studies to differentiate between independent molecules in the unit cell remains uncertain, and this a problem of paramount importance in modern X-ray crystallography.

Acknowledgements

We would like to thank the Australian Centre for Advanced Computing and Communications (ac3) for a grant in computing resources required for this work.

References

1 G. A. Jeffrey, J. R. Ruble and J. H. Yates, *J. Am. Chem. Soc.*, 1984, **106**, 1571.
2 M. R. Truter, *J. Chem. Soc.*, 1960, 997.
3 R. H. Blesssing, *J. Appl. Crystallogr.*, 1989, **22**, 396.
4 G. M. Sheldrick, SHELX-86. Program for crystal structure refinement, University of Göttingen, Germany 1986.
5 T. Kortisanszky, S. T. Howard, P. R. Mallinson, Z. Su, T. Richter and N. K. Hansen, XD—a computer program package for the multipole refinement and analysis of electron densities from diffraction data . Free University of Berlin, 1997.
6 M. J. Frisch, G. W. Trucks, H. B. Schlegel, G. E. Scuseria, M. A. Robb, J. R. Cheeseman, V. G. Zakrzewski, J. A. Montgomery, Jr., R. E. Stratmann, J. C. Burant, S. Dapprich, J. M. Millam, A. D. Daniels, K. N. Kudin, M. C. Strain, O. Farkas, J. Tomasi, V. Barone, M. Cossi, R. Cammi, B. Mennucci, C. Pomelli, C. Adamo, S. Clifford J. Ochterski, G. A. Petersson, P. Y. Ayala, Q. Cui, K. Morokuma, D. K. Malick, A. D. Rabuck, K. Raghavachari, J. B. Foresman, J. Cioslowski, J. V. Ortiz, A. G. Baboul, B. B. Stefanov, G. Liu, A. Liashenko, P. Piskorz, I. Komaromi, R. Gomperts, R. L. Martin, D. J. Fox, T. Keith, M. A. Al-Laham, C. Y. Peng, A. Nanayakkara, C. Gonzalez, M. Challacombe, P. M. W. Gill, B. Johnson, W. Chen, M. W. Wong, J. L. Andres, C. Gonzalez, M. Head-Gordon, E. S. Replogle, J. A. Pople, Gaussian 98, Revision A. 7, Gaussian, Inc., Pittsburgh PA, 1998.
7 C. Adamo and V. Barone, *Chem. Phys. Lett.*, 1997, **274**, 242.
8 R. F. W. Bader, *Atoms in Molecules a Quantum Theory*, Clarendon Press, Oxford, 1990.
9 F. A. Allen, O. Kennard, D. G. Watson, L. Brammer, A. G. Orpen and R. Taylor, *J. Chem. Soc., Perkin Trans. 2*, 1987, S1.
10 N. K. Hansen and P. Coppens, *Acta Crystallogr., Sect. A*, 1978, **34**, 909.
11 E. Clementi and D. L. Raimondi, *J. Chem. Phys.*, 38, 2686.
12 R. F. Stewart, *Acta Crystallogr., Sect. A*, 1976, **32**, 565.
13 S. T. Howard, FSTRUCT, an *ab initio* one-electron properties program, 1991.
14 S. T. Howard, unpublished results.
15 F. L. Hirshfeld, *Acta Crystallogr., Sect. A*, 1976, **32**, 239.
16 S. T. Howard, M. B. Hursthouse, C. W. Lehmann, P. R. Mallinson and C. S. Frampton, *J. Chem. Phys.*, 1992, **97**, 5616.
17 M. T. Carrol and R. F. W. Bader, *Mol. Phys.*, 1988, **63**, 387.
18 J. A. Platts, S. T. Howard and B. R. F. Bracke, *J. Am. Chem. Soc.*, 1996, **118**, 2726.
19 D. Zobel, P. Luger, W. Dreissig and T. Koritsanszky, *Acta Crystallogr., Sect. B*, 1992, **48**, 837.